Mohd Arif Ismail
Nik Mohd Ridzuan Shaharuddin
Omar Yaakob
Mohamad Hidayat Jamal
Faizul Amri Adnan
Ahmad Hadi Mohamed Rashidi
Wan Ahmad Hafiz Wan Mohd Azhary
Mohd Kamarul Huda Samion
Andiknurdiyana Bachok
Badruzzaman Ahmad
Nur Shafira Ahmad

WAKE WASH OF A FAST SMALL BOAT IN RESTRICTED WATERS: MODEL TESTS AND FULL-SCALE MEASUREMENTS

Summary

This paper presents the model testing of an 8.23m boat with hard chine planning hull generated waves at the Kilim recreational park. Wake is considered one of the main causes of riverbank erosion due to the energy carried by waves hitting the riverbank. Initially, ship particulars were measured from actual boats to generate a hull form using MAXSURF software. A lines plan was then generated to fabricate the model using fibreglass. Experiments were conducted in the National Hydraulic Research Institute of Malaysia (NAHRIM) at various speeds at a constant operating draft. The wave patterns generated by the modelled boats at different speeds were recorded for analysis. Wave attenuation for deep water conditions was studied and it was found that the wave exponent, *n* ranged from -0.36 to -0.75 for all depth Froude number (Fn_h) condition. Wave decay analysis was used to estimate wave height for defined water depth. For 11 people with an average mass of 65 kg on board, the produced wave height was greater than the permissible wave wake height of 75 mm. The generated energy exceeded 60 Joules/m for nearly all measured speeds. A boat speed of less than 5 knots was suggested for boats loaded with the maximum passenger limit of 11 people. Other recommendations were made to minimize the wave wake height produced by the modelled boat.

Key words: *Boat generated waves; Boat Wake Analysis; Wave attenuation; Wave energy*

Ismail, M.A., Shaharuddin, N.M.R., Yaakob, O. B.,
Jamal, M.H., Adnan, F.A., Rashidi, A.H.M., Azhary, W.A.H.W.M.,
Samion, M.K.H., Bachok, A., Ahmad, B., Ahmad, N.S.

Wake Wash of a Fast Small Boat in Restricted Waters: Model Tests and Full-Scale Measurements

1. Introduction

The Kilim Mangrove Park in Langkawi was listed as a UNESCO Geopark in 2007 and gazetted as "Protected Forest" under the Forestry Act of 1984. This listing has promoted the area as a tourist destination. Visitors to Kilim Karst Geoforest alone rose from 78,145 in 2006 to 240,817 in 2017. The increased number of tourists has, however, exerted excessive demand on the environmental ecosystem of the Kilim Karst Geoforest Park and threatened the sustainability of this area for tourism. The impact of vessel generated high waves has negatively affected the ecosystem, particularly its mangrove forest through the critical erosion experienced by its riverbank. As the ecotourism industry in Malaysia is becoming the main source of income for people living in waterway areas, the preservation of mangrove ecologies and the river environment has to be given serious consideration.

Among the main creators of high waves are speeding tourist boats. Most of the touring activities boat today belongs to the hydrodynamically support classification [1]. According to the ITTC High-speed marine vehicles are classified as vessels with a design speed equivalent to a Froude number more than 0.45, and/or a speed greater than $3.7\nabla^{0.1667}$ m/s, and/or when high trim angles are expected, or for dynamically supported vessels [2]. Several researchers relate the erosion experienced by the riverbank to the wave wake produced by the high-speed boat. In the Mississippi River for instance, Johnson investigates the shoreline erosion rate in relation to the water turbidity induced by the recreational boat wake. They reported that recreational boating on the Mississippi River Main Channel is the contributing influence most responsible for the documented high rate of shoreline erosion [3]. Kirkegaard et al. developed a criterion based on their experimental data from their research perspective in Denmark's coastal area [4]. Hence, the Danish Maritime Authority issued a governmental order requires the HSC owner/operator to document that the ship-generated waves do not exceed the criterion of $H_h \leq 0.5\sqrt{\frac{4.5}{T_h}}$ where H_h is is the maximum wave height (in meters) of the long periodic waves having the mean wave period in T_h (in seconds) [4]. In Gordon River, Nanson et al. conducted a series of boat wake experiment in relation to the bank erosion rate [5]. They demonstrated that the variations in the river's flow were not the result of any significant changes in flow regime, but rather a reflection of the significant influence boat wakes may have on river-bank erosion. Macfarlane and Cox developed a new Noosa and Brisbane River wave energy criterion [6]. The allowable criterion is that the energy from the vessel's maximum wave height cannot exceed 60 Joules/m for the Noosa River and 180 Joules/m for the Brisbane River, respectively. Ahmad et al. conducted an experiment in an eroded mangrove region in the Kemaman River estuary to determine the link between wave train energy and maximum wave energy produced by the boat [7]. Macfarlane produced an empirical tool in 2012 that can predict the characteristics of the wave wake generated by boats quickly and precisely, as well as suggest and incorporate a wave wake regulating criterion as an added solution to the erosion issues into their prediction tool [8]. In the Vietnamese Mekong Delta province of Ca Mau, La et al. perform a series of boat wave wake effect to the bank's experiments. They came to the conclusion that bank failures occur when the boat-induced shear stress acting on the riverbank exceeds the soil's critical shear stress. They also illustrate that plants can act as a bank protection system [9]. This includes other researchers [10] [11] [12] seeking the effect of the boat wave wake to their respective area of interest, particularly its riverbank erosion which located at the sheltered waterways.

Wake wash is a natural phenomenon that happens when a vessel moves over calm water, which causes the formation of waves profile on both sides of the vessel. It is noted that the wave profile carries a certain amount of energy, which if sufficiently high can affect riverbanks in riverine, canal, or waterway areas such as Kilim River, Langkawi. To be specific, riverbank

erosion due to wave wash is an issue that needs to be addressed. Some of the factors that characterize wave wash are the number of boats and its lateral position moving along a river during certain period of time, the hull form and speed of these boats, and the depth of the river. The characteristics of these waves are altered significantly with changes in speed, water depth, and hull form [13]. According to Ghani and Rahim, there are two sets of waves, which are divergent waves that move out at an angle from the centreline of travel and transverse waves that move out from the stern perpendicular to the centreline of travel. Both of these waves carry a certain amount of energy that affects their surroundings [14]. These waves can be easily seen from a moving vessel as shown in Figure 1.
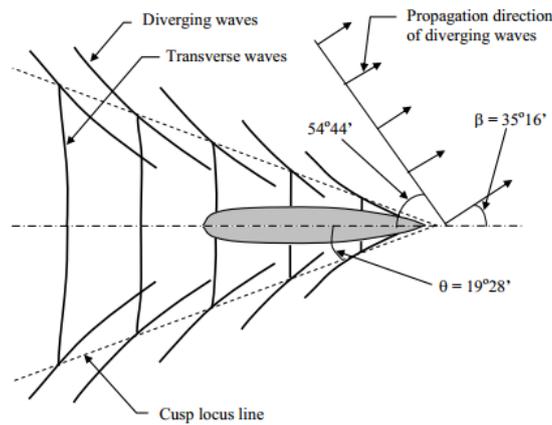
Fig. 1 Kelvin wave pattern [8]

Vessel wave wake is frequently defined into three categories, based on vessel speed at its corresponding water depth. The depth Froude number, Fn_h, which is a nondimensional relationship between vessel speed, V and water depth, h is defined as in Equation 1:

$$Fn_h = \frac{V}{\sqrt{gh}} \tag{1}$$

Where:

    V = vessel speed (m/s)

    g = gravitational acceleration, (9.81m/s^2)

    h = water depth (m)

In general, speed regimes are categorized as critical when $Fn_h = 1.0$, sub-critical for $< Fn_h = 1.0$, and super-critical for $> Fn_h = 1.0$. According to Macfarlane, more classified Fn_h can be made for sub-critical region. For $0.75 < Fn_h < 1$ will be the trans-critical regimes which is very near to critical [8]. While $Fn_h < 0.75$ will be the absolute sub-critical region. The wave wakes are beginning to spill in the spanwise direction in the form of Kelvin waves, as the Fn_h increase [15].

Thus, studying the effect of boat generated waves in rivers is important because some rivers such as Kilim River have shallow water and narrow channels at certain locations. In short, research on the environmental impact of the waves generated by tourist boats is important because of their damaging effects over the long run. As the tourism industry in Malaysia contributes to the nation's economy and part of the population depends on tourism for their livelihood, careful studies should be done on boats speeds and wave energy to minimize the impact of boat generated waves on riverbank erosion.

Ismail, M.A., Shaharuddin, N.M.R., Yaakob, O. B.,   Wake Wash of a Fast Small Boat in Restricted Waters:
Jamal, M.H., Adnan, F.A., Rashidi, A.H.M., Azhary, W.A.H.W.M.,   Model Tests and Full-Scale Measurements
Samion, M.K.H., Bachok, A., Ahmad, B., Ahmad, N.S.

This paper investigates the boat wake characteristics of 27 feet (8.23m) boat which is commonly used in Kilim River. By comparing with the available international criteria, this study assesses the boat generated waves by conducting both full scale measurements and laboratory scale tests. This will provide a basis for the development of Kilim River own allowable wake criterion in the future.

2. Research Approach and Methodology

2.1 Full-Scale Measurement

2.1.1   Area of Interest Location in Kilim River

Figure 2 shows the google map of Kilim River, with locations for site measurements labelled from A to G. A set of data regarding Kilim River bathymetry, width and water depth was obtained from the National Hydraulic Research Institute Malaysia (NAHRIM) (unpublished). The data shows the river width ranges from 30m to 66m and water depth of 2.3m to 5m at nearly all area of interest. The smallest river width of 30m and 2.3m water depth is located near the Gua Kelawar (G), one of the most critical banks that undergoes the erosion. Other critical location pins pointed A, B, C, and D having the river width of 48m to 66m with a water having an average depth of nearly 4m. Control location of E and F (not a boat route for tourist activities) width is from 30m to 40m with a water depth range from 2m to 4m.
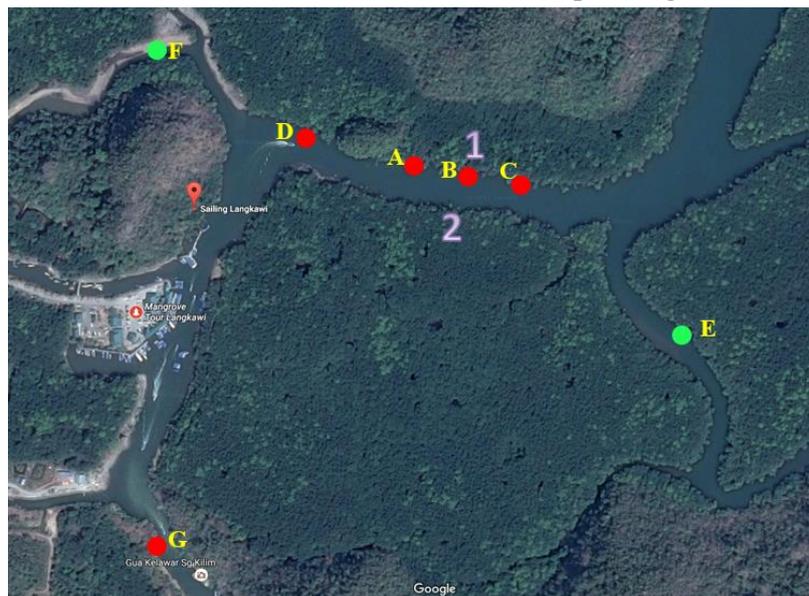
Fig. 2 Kilim River maps location of interest

The bottom bathymetry of the Kilim River riverbank for the cross-section B (6° 24' 23.627", 99° 51' 41.449") is shown in Figure 3. For the full-scale measurement (Section 2.2) the boat tested was heading from cross section B to cross section A; with an average water depth of 4m.
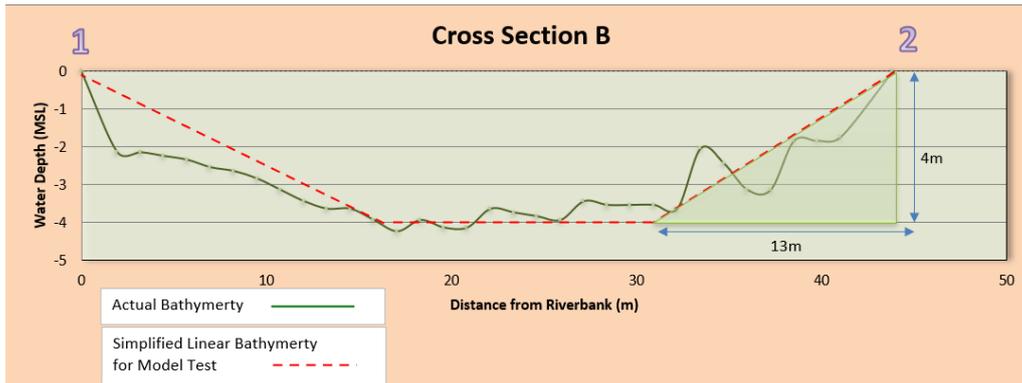
Fig. 3 Bathymetry – cross section of one of the pin point interest location (B), data source: NAHRIM

2.1.2   Hull Form Selection and Field Testing

The boat with 8.23m length overall is shown in Figure 4 was chosen for the full-scale measurement as this type and size forms the majority (more than 60%) of the boats owned and used in Kilim River tourism activities.

Fig. 4 Dynamic maker hull form

Tide gauges were used to measure the boat wave wake in this research. The calibrated device; RBRsolo D|tide gauge has the ability to record wave heights continuously at a frequency of 2 Hz and the values of water elevation were later analyzed to derive the wave parameters produced by the boat. The tide gauges were installed on sturdy steel frames as shown in Figure 5 [16]. Operating under intermediate water depth condition and limited by the slope condition of the bank, this tide gauge was located at a distance of 3m from the riverbank and positioned at least 1.5m under the mean water level surface to obtain an accurate and good reading. The positioning took into account the tidal range for the tide gauge deployment and measuring process during the experimental work. The water depth and the tide placement under water were measured by Laylin Speedtech SM-5 Depth meter Water Portable Sounder; Depth Meter device. The distance from the riverbank were measured by using Makita LD050P Laser Distance Measurement device.

Fig. 5 Tide gauge (not visible – submerged under water) installed vertically on blue steel frame

The schematic diagram of the full-scale measurement is shown in Figure 6. 65kg sand bags were used to represent the mass of people onboard. To maintain the deep-water condition, all test runs were conducted during the highest tide. Four runs were made for each speed. The boat speed and sailing line distance of the boat is monitored with the aid of GPS. To prevent the gauge from recording waves while the boat is in acceleration speed, the touring boat has to be at certain starting line distance from the tide gauge in order to achieve a desired constant speed. The starting line has to be at least 120m for trans-critical and super-critical speed while at least 40m for sub-critical speed. This distance ensures the boat is travelling in straight and approximate sailing line distance to the tide gauge. Since the boat is operated under full 11 person onboard represented using the sand bag, the desired speeds especially high speed of higher than 8knots has to be increased steadily taken into account for actual person safety which is the operator and two record keepers.
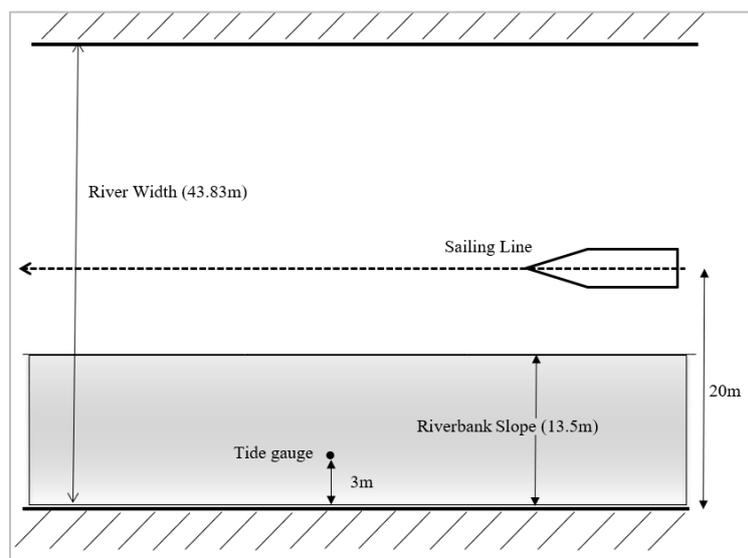
Fig. 6 Schematic Diagram for Full-Scale Measurement

2.2 Model Test Procedures

2.2.1   Model Boat Construction

The model size glass reinforced fibre boat was scaled down using a 1:7 ratios from a full-scale length of 8.23m based on the available working length and width of the NAHRIM facility. The hull form was generated based on a digital representation of an actual 8.23m boat measured during field work. Measurements were carried out using a Makita LD050P laser measuring device and data was taken from 11 different stations. Based on this data, the hull form was generated using the MAXSURF Fitting module, before proper fairing and adjustments were made using the MAXSURF Modeller. The lines plan produced from the measurement is shown in Figure 7.
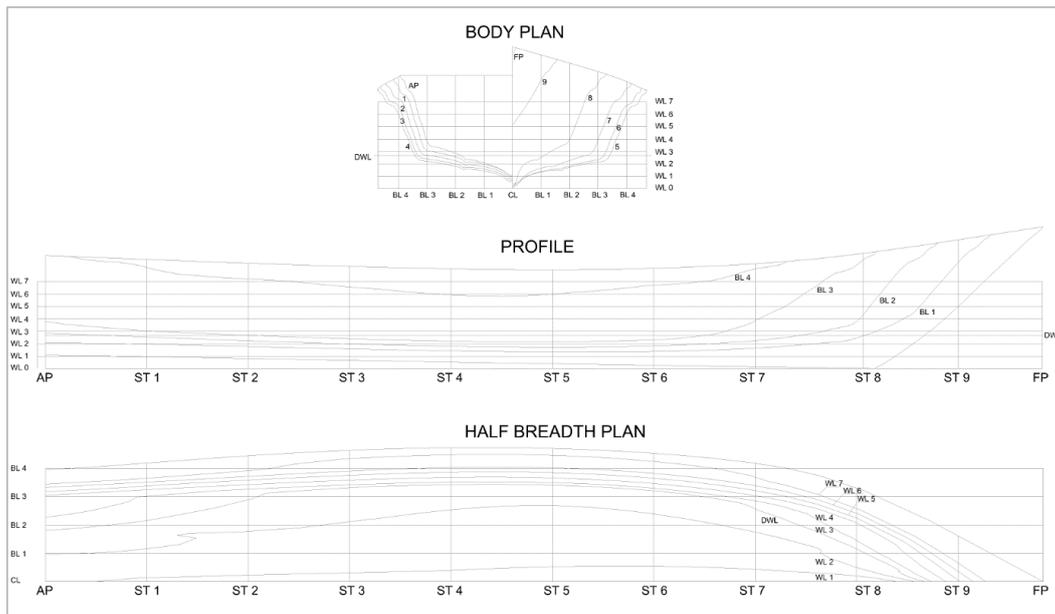
Fig. 7 The lines plan of the 8.23m Kilim River boat

The boat parameters for the full and scaled model are shown in Table 1. The Froude number (Fn_h) and law of similarity were used to calculate model speed and mass displacement, respectively.

Table 1 Model Boat Parameters

Parameters	Model Scale	Full Scale
Boat Length Overall, LoA (m)	1.18	8.23
Boat Length waterline, L_{wl} (m)	0.99	6.95
Breadth, B (m)	0.30	2.12
Depth, D (m)	0.16	1.12
Draft, T (m)	0.04	0.29
Displacement (kg)	3.5	1210
Hull Speed (knots)	2.44	6.46

The total mass of the boat model including a battery, controller, and propulsion system was 3.5 kg, which is equivalent to a full-scale boat with 11 passengers. The boat was powered by a small 14.8 V battery, which provided the minimum voltage required for the model scale boat to move at the desired speed during the laboratory tests. Figure 8 and Figure 9 show the model during the construction stage and the arrangement of propulsion system, respectively.

Fig. 8 Construction of the model hull form   **Fig. 9** Equipment arrangement
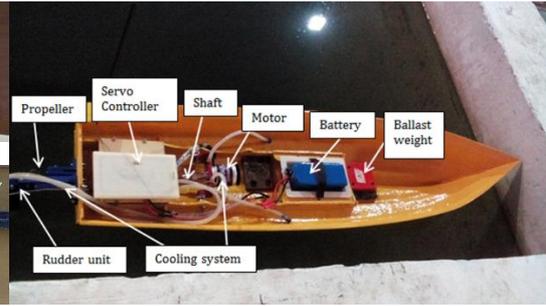
2.2.2   Coastal Wave Basin Setup

The ship generated wave (SGW), or wake experiment was conducted in the Coastal and Estuarine facility at the NAHRIM. The length, width, and depth of the coastal wave basin were 53m, 30m, and 1.2m, respectively. The NAHRIM wave basin has a maximum water depth of 0.8m. Under the 1:7 scale, 0.6m water level was setup to resemble the average 4m water depth conditions during the full-scale tests in Kilim River. Only half of the total area was used in this research since the space was adequate in preventing the reflection of boat generated waves from area walls. To resemble the real river conditions, a slope was constructed in the coastal wave basin as shown in Figure 10. This resembled the slope of the riverbank and bed at Kilim River according to NAHRIM bathymetry data from the selected location from Figure 2. The slope had a 17.7° angle, 15m distance, and was simplified to a straight line as previously mentioned in Figure 3.

Fig. 10 Slope setup under preparation at NAHRIM facility for model testing

Five resistance wave probes were used to obtain the wave generated waves during model tests. For deep water condition, the Wave Probe 6 and Probe 2 were attached to this region as in Figure 11. The intermediate water condition from the slope function is where the wave Probe 3, Probe 4 and Probe 5 were located shown in Figure 12.
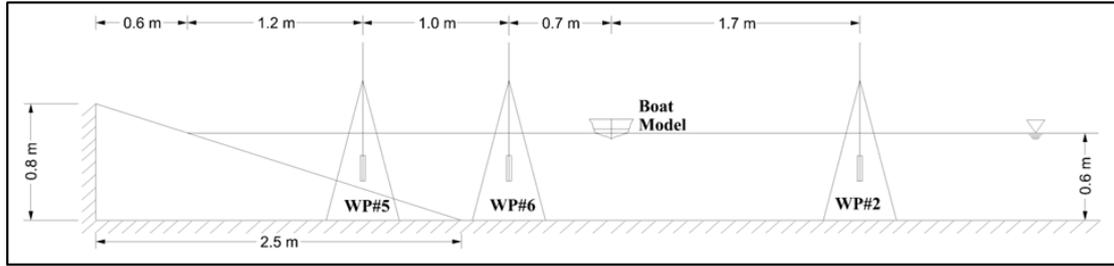
Fig. 11 Slope setup for model testing in NAHRIM
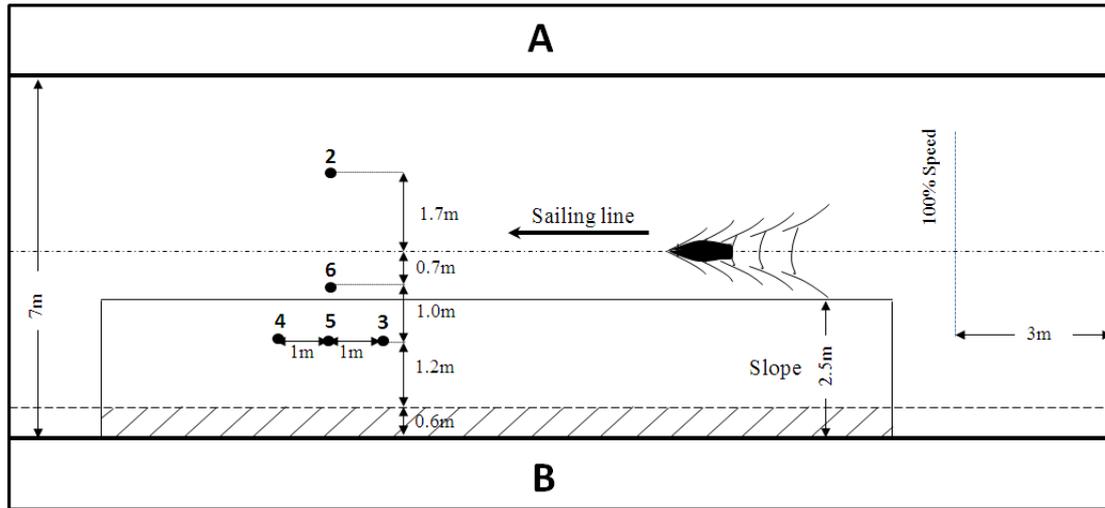
Fig. 12 Schematic Test Procedure Diagram (Numbers Indicate Wave Probes)

2.2.3   Model Test Wave Data Assessment and Test Protocol

During model tests, one of the study limitations is that wave probes could not be located exactly at the same corresponding location as in the full-scale test because the relatively large size of the probe holder prevented probes from being installed close to the 'shore'. The location of the wave probes is shown in the schematic diagram in Figure 12. Wave Probe 3, Probe 4, and Probe 5 were arranged in a straight line parallel to the sailing line. These wave probes were expected to have similar wave heights, with appropriate time delays. Wave Probe 2 was arranged as a mirror to wave Probe 5 on the opposite side of the sailing line. Before starting any test, the wave probes were first calibrated. 20 seconds were allocated to measure each run with data acquisition frequency of 50Hz. Figure. 13 shows the wave probe locations as well as the starting and finishing lines. As mentioned in Section 2.1, the model scale boat was powered by an electric propulsion system and was capable to achieved a constant highest speed tested as the boat enters the starting line. This starting and finishing lines were separated by a distance of 13 meters.

Ismail, M.A., Shaharuddin, N.M.R., Yaakob, O. B.,   Wake Wash of a Fast Small Boat in Restricted Waters:
Jamal, M.H., Adnan, F.A., Rashidi, A.H.M., Azhary, W.A.H.W.M.,   Model Tests and Full-Scale Measurements
Samion, M.K.H., Bachok, A., Ahmad, B., Ahmad, N.S.

Fig. 13 Wave probe locations and model testing distance line at NAHRIM facility

2.2.4 Speed Measurement

As the model scale boat did not have a speed logger, the model speed was manually measured. Boat speeds were calculated from the duration it took for the boat to travel from the starting line to the finishing line as indicated in Figure 13. These speed tests were repeated several times to obtain average speed data with an error range from ±0.01 to ±0.06. The boat was also tested at slower speed to see the effect of low speeds on boat generated waves. Figure 14 shows a typical test run, with wave probes located near the slope. Wave wake data from wave probes were fed directly into the NAHRIM facility data acquisition system. Each probe was connected to the data acquisition system via an input channel, which was numbered according to the probe number.

Fig. 14 Typical Test at NAHRIM Facility

3. Results and Discussion

3.1 Kilim River boat generated waves characteristics

3.1.1   Full Measurement Wave Height Data

Figure 15 shows the fields measurement data of the boat at the sailing line distance of 20m. This data shows an agreement to other researchers' data [8][17][18] for estimating and assessing the high-speed craft. Error value from the full-scale experimental work was estimated between ±0.003 to ±0.006. Since the on-site bathymetry was not uniform in this experimental work, the produced wave height and its corresponding period varied. The wind generated waves and the tidal current direction (downstream or upstream) might affecting the wave height measured when conducting the experimental work. Noted that, the measurement was done within a small range (less than 0.3m) of water depth difference due to tidal movement.
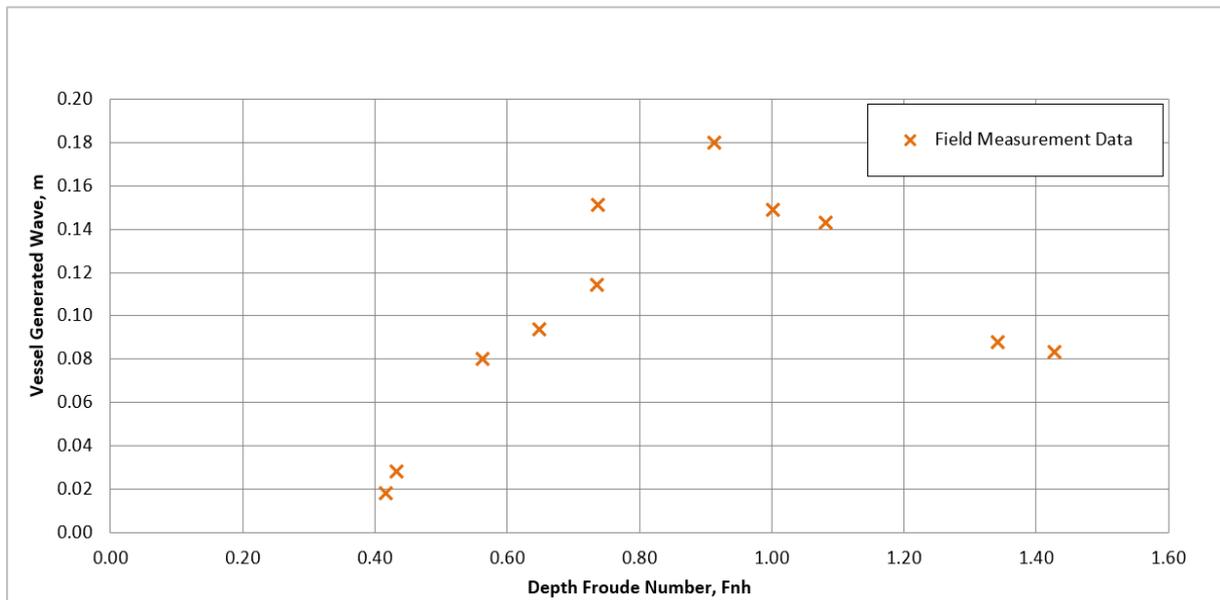
Fig. 15 Full measurement wave wake heights at various Fn_h

3.1.2   Model Testing Wave Height Analysis

3.1.2.1 Boat Generated Wave (Wake) Depth Froude Number Fn_h

Boat wake conditions were presented according to the depth Froude number (Fn_h). Table 2 shows the speeds and Fn_h for each run. Depth Froude number (Fn_h) criteria were used to determine whether a boat was in sub-critical, trans-critical, critical or super-critical conditions. Critical Fn_h was expected to produce the largest wave wake height and the highest wave energy. However, the critical speed for (Fn_h=1) is quite difficult to get due to the speed control limitation. Thus, the Fn_h critical value of 1 is not included in this study. Table 2 shows the speed and its corresponding Froude Number for the tests.

Ismail, M.A., Shaharuddin, N.M.R., Yaakob, O. B.,   Wake Wash of a Fast Small Boat in Restricted Waters:
Jamal, M.H., Adnan, F.A., Rashidi, A.H.M., Azhary, W.A.H.W.M.,   Model Tests and Full-Scale Measurements
Samion, M.K.H., Bachok, A., Ahmad, B., Ahmad, N.S.

Table 2 Speed and Depth Froude Numbers during the tests

Model scale		Full scale	Depth Froude No.	Condition
(m/s)	(knots)	(knots)	(Fn_h)	
1.33	2.59	6.84	0.549	Sub-critical (Fn_h <0.75)
1.87	3.63	9.6	0.769	Trans-critical (0.75< Fn_h <1)
2.13	4.14	10.98	0.880	
3.52	6.84	18.08	1.449	Super-critical (Fn_h >1)
4.18	8.13	21.52	1.725	
4.25	8.26	21.85	1.751	
4.25	8.26	21.87	1.753	
5.05	9.82	25.96	2.081	
5.06	9.84	26.05	2.088	

3.1.2.2 Wave Height Error Estimation

Under the same measured speed, the error of the wave height produced was expected as the wave train (packet) developed. Several factors related to producing these errors such that, the ability to keep the sailing line distance to the wave probe as the model scale vessel travel relied on human controller not by the towing carriage facilities which is not available in NAHRIM. As well as keeping the desired speed ideally constant all the time during the measurement period. For one wave train, the maximum wave occurred at different period of wave oscillation. Where by the maximum wave height appeared in the fourth wave period while others may appear at the later than fourth period wave. The percentage error estimated in the maximum wave occurred during the fourth period wave was in the range of 3% to 12% while 7% to 11% error is expected when the maximum wave occurred during the later period wave. From the maximum wave height magnitude, the percentage error range was from 1.6% to 6%. The rest percentage error for the remaining individual wave after the maximum wave height occurrence in the wave train varied in a larger magnitude due to the dispersion. These remaining waves within the packet have rather low potential in inducing the riverbank stability compared to the maximum wave height possessed in the packet. In this paper, focus was given to the maximum wave height as a respond to their respective wave energy that been produced.

3.1.2.3 Model Wave Height Production under Operating Mode

Comparisons wave height data obtained from the model testing between wave Probe 5, Probe 6, and Probe 2 are shown in Figure 16. It shows the wave height of the modelled boat conditions characteristics associated with the displacement, transition (semi-planning), and planning speed modes. These modes represented with the speed of the boat or its Fn_h. For this model testing, speeds lower than 3.5knots, the model boat experienced sub-critical conditions. While at between 3.5knots to nearly 4.7knots, experienced trans-critical condition and for the speed larger than 4.7knots, it is under the super-critical condition. According to the trend line (red dotted) for all measured waves, the largest produced wave height was when Fn_h approached 1. Images of the produced waves were also taken to differentiate the wave angle produced under these several speed modes and Fn_h conditions.
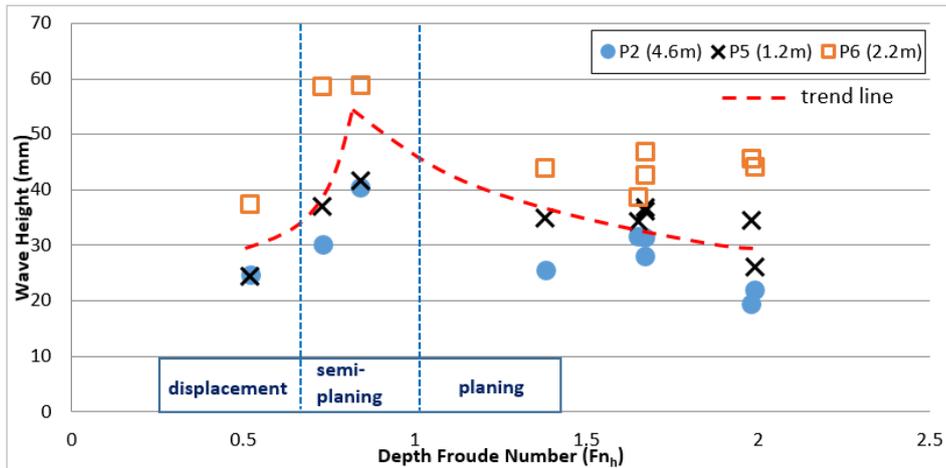
Fig. 16 Model scale wave heights at different probe locations

In displacement (left) mode or $Fn_h < 0.75$ the wave height produced by the model testing is lower compared to the other two modes. As in this mode, the speed is at the lowest the boat can be operated with, less power required and the bow down in the water. The observed wave angles in Figure 17 obtained from three-dimensional image processing measurement were in the range of 20° to 30° for this sub-critical condition. The transverse wave was clearly visible at a small amplitude.

Fig. 17 Displacement mode; run speed of 2.59knots for Sub-critical condition $Fn_h = 0.55$

In the transition or semi-planning (middle) mode ($0.75<Fn_h<1$) where the boat encountered more resistance from increases in its wetted hull area; under the condition where the stern to plow more in the water as its bow rise, bigger wave generation produced from this condition. The increment of the wave height to its maximum value discovered under this speed mode. Wave generated profiles for this condition shown in Figure 18. The angle for trans-critical Fn_h is slightly bigger than the sub-critical conditions, larger than 30°. Where else the wave amplitude started to increase to its nearest highest value the model boat able to produce and the divergent waves started to become more dominant than the transverse waves.

Ismail, M.A., Shaharuddin, N.M.R., Yaakob, O. B., Jamal, M.H., Adnan, F.A., Rashidi, A.H.M., Azhary, W.A.H.W.M., Samion, M.K.H., Bachok, A., Ahmad, B., Ahmad, N.S.

Wake Wash of a Fast Small Boat in Restricted Waters: Model Tests and Full-Scale Measurements
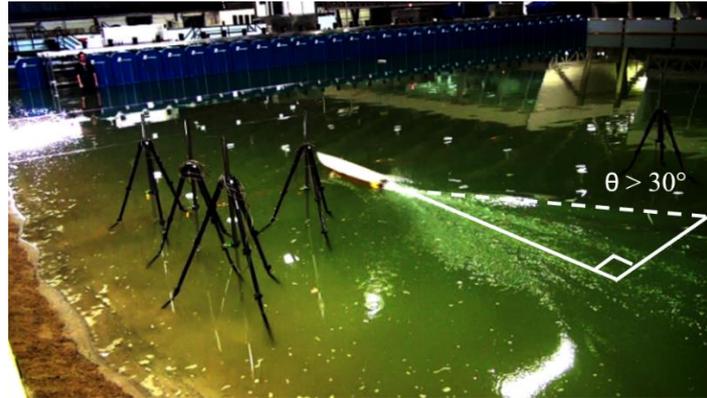
Fig. 18 Semi-planing mode; run speed of 3.63knots for Trans-critical condition $Fn_h = 0.77$

As the boat in planing (right) mode, speed increased to the Fn_h of larger than 1. The boat wake produced became smaller because in this region, the bow drops down into the water. But due to the high speed the boat operated, it is hydrodynamically supported by both buoyancy and lift forces which put the hull in position [19] as can be seen in the Figure 19. The observe wave angle for super-critical was found between 4° to 10°. The hull contact to the water is at its minimum, the wave height produced is smaller than semi-planing mode but slightly higher than the displacement mode. It was observed that during this super-critical condition, only the divergent wave visible.
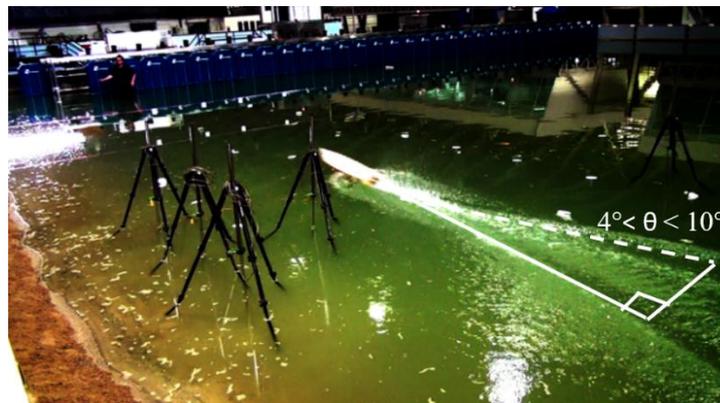
Fig. 19 Planing mode; run speed of 9.84knots for Super-critical condition $Fn_h = 2.088$

From water wave dynamic point of view, Probe 6 and Probe 2 were located in the deep-water condition; the generated wave base does not feel the bottom. Probe 6 has the highest wave height due to its distance of 0.7m which is nearer to the model boat sailing line compared to Probe 2 which is farther at 1.7m as seen in Figure 12 previously. These probe 6 and 2 will be used further in estimating the wave decay of this particular touring boat.

Meanwhile Probe 5 located at the intermediate depth where the wave base start to feel the bottom slope and have significant changes to the height produced. This Probe 5 is the mirror of Probe 2 whereby it has the same distance from the sailing line which is 1.7m. However, the waves passing through Probe 5 showed higher wave height magnitudes than waves passing through Probe 2 (placed at deep water condition) because of the effect of water depth. The slope was considered a shoaling zone that increased wave height while altering the length of incoming waves. The wave decay technique explained in Wave Decay Finite Depth Envelope Analysis sub-section was used to estimate the wave heights produced at an exact field measurement location.

It was noted that wave probes 3, 4 and 5 along a line parallel to the direction of the boat experienced the same wave pattern. Figure 20 shows the wave heights taken from three different wave probes aligned with the direction of a boat travelling at 8.26knots. The wave patterns for these wave probes were very similar, albeit with time shifted.
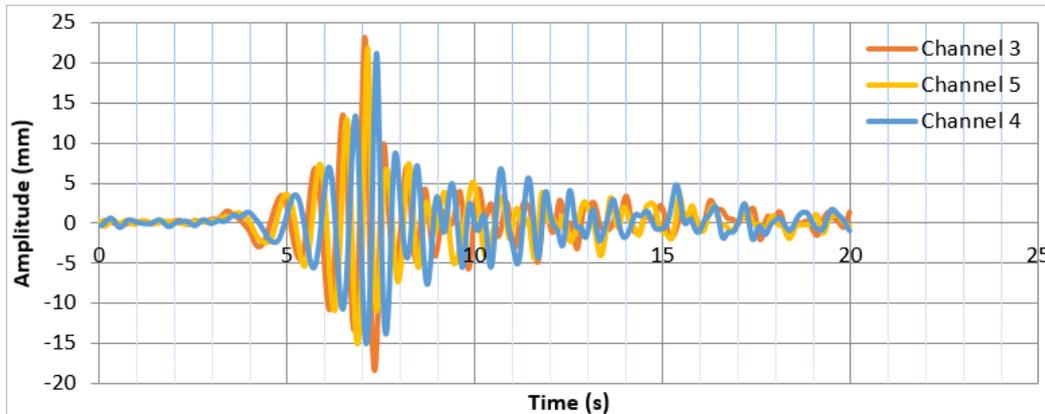
Fig. 20 Wave heights with respect to time for three different in-line Wave Probe 3, Probe 5 and Probe 4 (red line Channel 3; yellow line Channel 5; blue line Channel 4)

3.2 Model Testing Wave Attenuation Estimation

3.2.1 Wave Decay under Deep-Water Condition

Vessel generated waves propagate at unique angles for different depth Froude numbers (Fn_h) as seen in Figure 16-18. The Kelvin wave patterns for deep water conditions in sub-critical regions had a wave angle of 19°28' while the propagation angle of the diverging waves was 35°16'. According to Havelock [20], depth Froude number (Fn_h) increases from subcritical to critical conditions from 19°28' to 90° and decrease exponentially from critical to super-critical conditions from 90° back to 19°28' as shown in Figure 21.
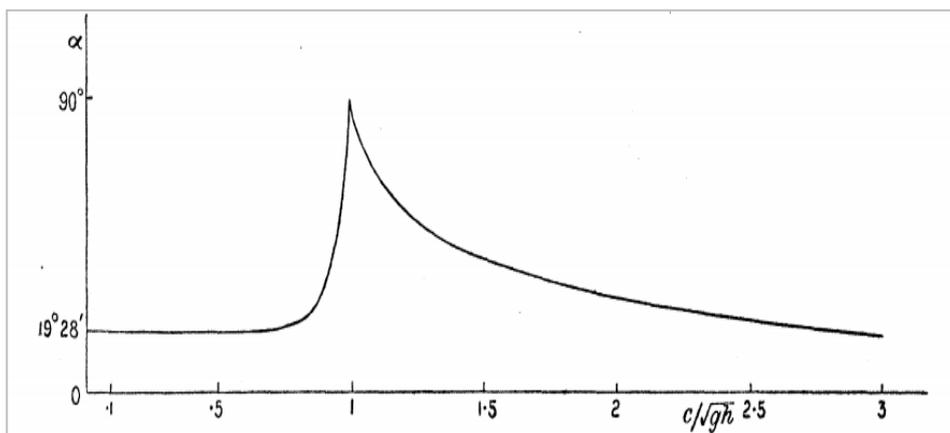
Fig. 21 Wave angle, θ as a function of $Fn_h = V/\sqrt{gh}$ [20]

As the wave wake travels from the vessel to shore, wave heights or amplitude decreased and the waves intensity diminished with a distance. This wave attenuation analysis used the wave decrement condition to estimate wave height at any lateral position from the sailing line of the vessel. Macfarlane [21] suggested that measurements be made at a minimum of four lateral locations within regions between 1.5L to 3.0L.

Wave decay can be estimated from wakes in the deep-water conditions. Main analysis parameter used the decay rate of the divergent wave produced by the vessel. Havelock [20]

Ismail, M.A., Shaharuddin, N.M.R., Yaakob, O. B.,   Wake Wash of a Fast Small Boat in Restricted Waters:
Jamal, M.H., Adnan, F.A., Rashidi, A.H.M., Azhary, W.A.H.W.M.,   Model Tests and Full-Scale Measurements
Samion, M.K.H., Bachok, A., Ahmad, B., Ahmad, N.S.

discovered that wave amplitude on the cusp line of a diverging wave system decays at a rate proportional to the inverse cube root (n = -1/3) of the distance from the sailing line in deep water while transverse wave attenuation exponents n is -1/2. This was later used by Renilson and Lenz [22] to develop a lateral distance-independent approach for measuring vessel wash. They observed that the maximum wave height (H) of a vessel may be estimated for a given offset from the sailing line (y), once wave height constant, gamma (γ), and the decay coefficient (^{n}) in Equation 2 is known. Hence, the wave curve in the power form of Equation 2 was obtained from experimental data:

$$H = \gamma . y^n \tag{2}$$

Where:

H = wave height (m)

γ = wave height constant

y = sailing line distance (m)

n = decay coefficient

In this research the lateral locations of interest were less than 2.0L due to a small river width relative to the full boat length, which limits the sailing lines distance to the riverbank. In addition, wave probes could only be located at two lateral positions. By comparing tolerances obtained from Macfarlane [8], a realistic judgment was made for this study's model testing data. Wave height and lateral distance were divided by boat model length to obtain non-dimensional values as shown in Figure 22.
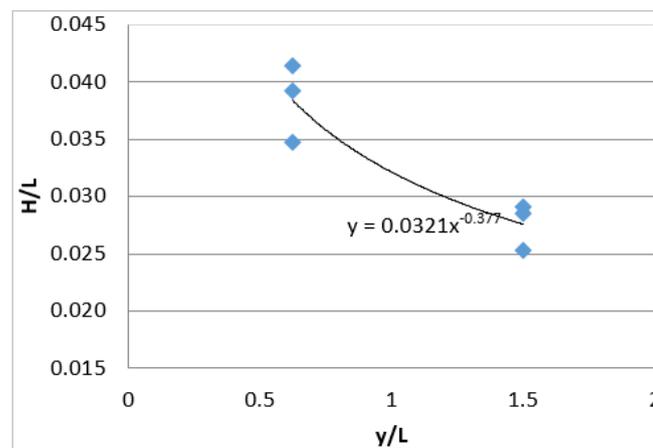
Fig. 22 Analysis of wave height constants in super-critical condition (Fn_h = 1.67)

Only using two points of lateral distance may not allow the power curve to predict accurate wave exponents and height constants. Wave decay in deep water has been proven to exponentially decrease of at least -0.33 for conservative approximation for high-speed craft [23]. By comparing several lateral distance values for 0.62L to 1.86L from the literature [21], the wave height tolerance constant, γ was found to average ±2.02% while the wave exponent (n) had an average tolerance of ±3.66%. Another analysis was done using the MAXSURF 20.06 V8i software. MAXSURF is a well-known program used by naval architectures, engineers, and academicians in the marine industry [24]. One of the modules in MAXSURF [25] is MAXSURF Resistance, which provides a wide range of resistance calculations for several types of vessels, including planing vessels. Resistance estimation using MAXSURF software shows a fair agreement in term of the solution parameters when compared to the CFD approach [26]. Another comparison has been made with the wave wake predictor developed by Macfarlane et al. [27] where the MAXSURF Resistance software predicted wave wake magnitude with a less

than 5% error. By adapting the potential flow calculation over the hull, MAXSURF able to calculate the wave surface elevation value with the aid of changing contours. The free surface analysis was utilized to find the longitudinal wave cut at various lateral distances from the sailing line. The free surfaces were first run under several grid points for numerical convergence check as refer to Wang [28] approach in order to verified the computed data obtained. Figure 22 shows the numerical convergence check of several grid points of the computed free surface data. Several grid points were used to find the optimum wave wake data from the computed free surface in MAXSURF resistance. The analysis required a set of less than 700 number of each grid from longitudinal and transverse grid. The front grid flow starts from at least 2 times boat length upfront, and heading towards the boat hull to the transom. At least 8 boat length grid distance were used to obtained the computed free surface behind the boat trail while 4 boat length distance at both port and starboard side of the vessel.
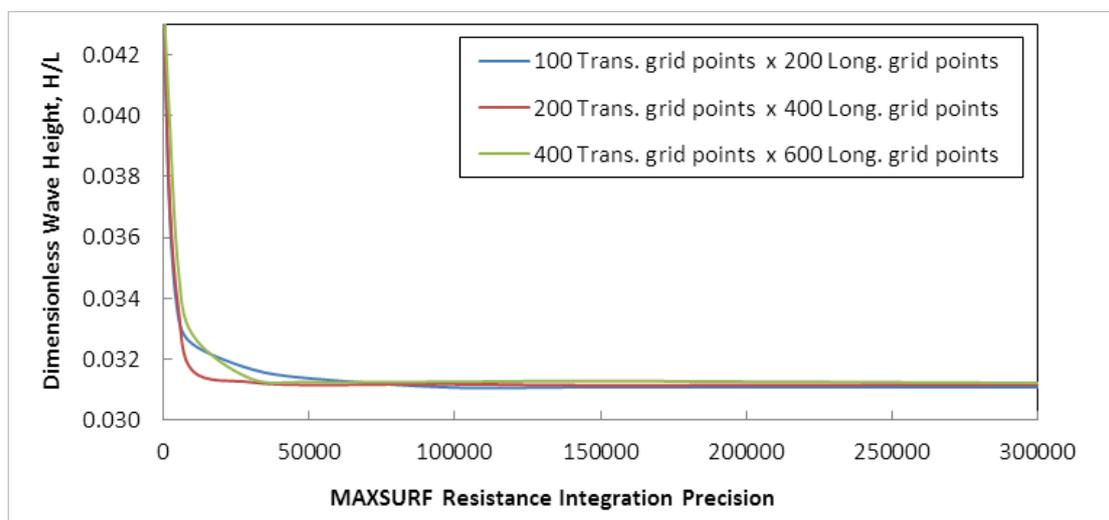
Fig. 23 Numerical convergence check on MAXSURF computed data

This convergence checks were performed in domains of a higher grid points (400 x 600) to be compared to a lower grid point of 100 Trans. times 200 Long. grid points. The numerical convergence is confirmed by the convergence of the dimensionless wave height data as in Figure 23 above.

The free surface of the boat computed by the MAXSURF resistance software is shown in Figure 24. It is noted that the waves produced in the simulation had patterns and angles similar to the waves produced in the experimental work.

Table 3 shows the wave height constants (γ) and respective exponential constants (n), with adjustments for margins and MAXSURF software computed data. The wave height constant, γ showed good agreement between the model tests and computed values. Using non-dimensional values, the difference was less than 13.65%. The computed wave decay exponential (n) value indicated larger differences for both sub-critical and super-critical condition of 26.4% to 76.2% while for trans-critical conditions the difference was only 4%. This big difference, especially for sub and super-critical conditions, was expected due to Thomas et al. [29] showing the exponential values ranging from -0.2 to -1.0. The wave exponential (n) values from their study were simplified into one trend line for comparison with this study's experimental and computed values as shown in Figure 25. Note that the literature's scattered value is not shown in this Figure 25, where only simplified trendline were shown.

Ismail, M.A., Shaharuddin, N.M.R., Yaakob, O. B.,
Jamal, M.H., Adnan, F.A., Rashidi, A.H.M., Azhary, W.A.H.W.M.,
Samion, M.K.H., Bachok, A., Ahmad, B., Ahmad, N.S.

Wake Wash of a Fast Small Boat in Restricted Waters:
Model Tests and Full-Scale Measurements

a)   Sub-critical Conditions

b)   Trans-critical Conditions

c)   Super-critical Conditions
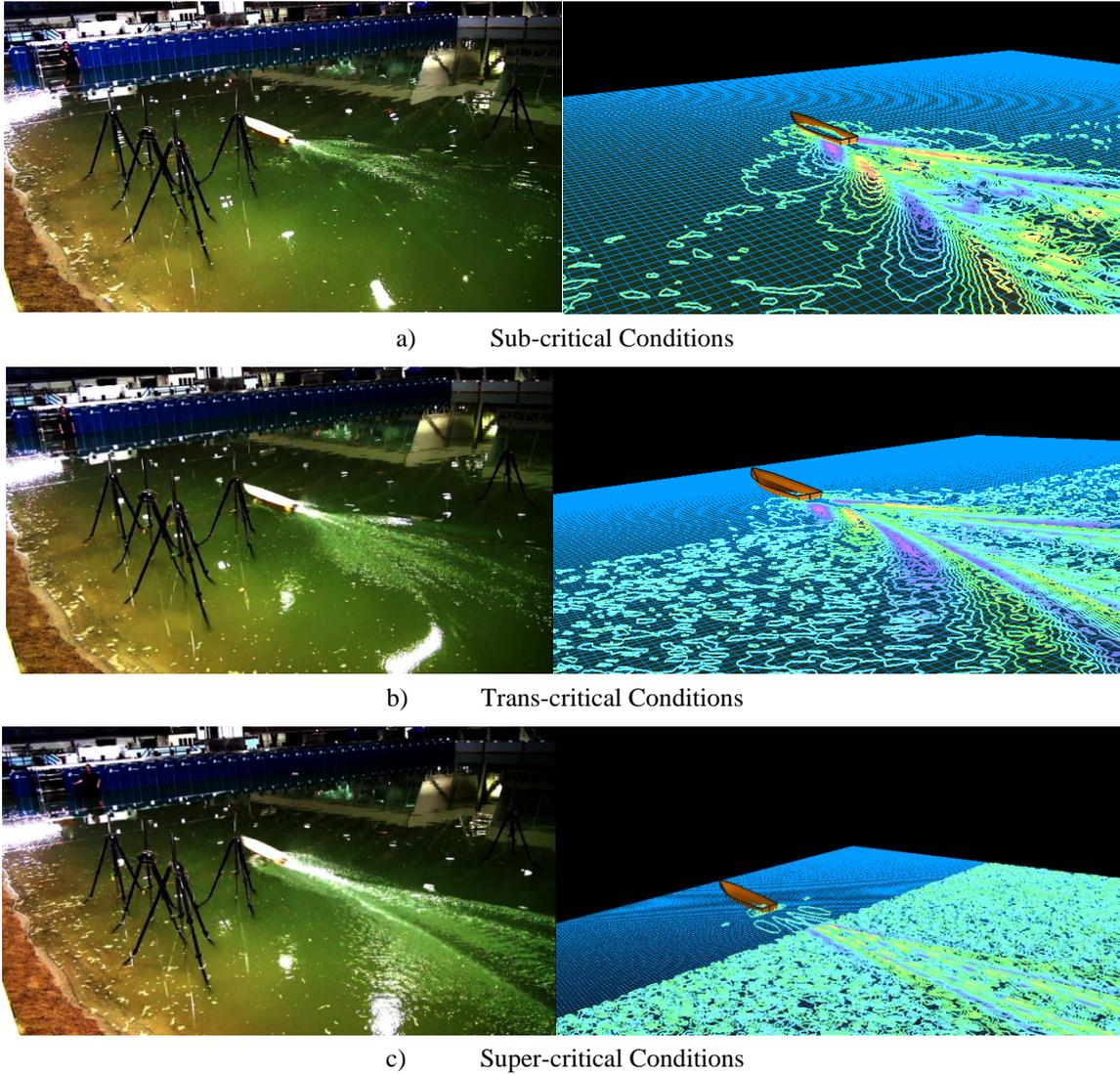
Fig. 24 Boat generated waves comparison between experimental and computed data for three Fn_h conditions
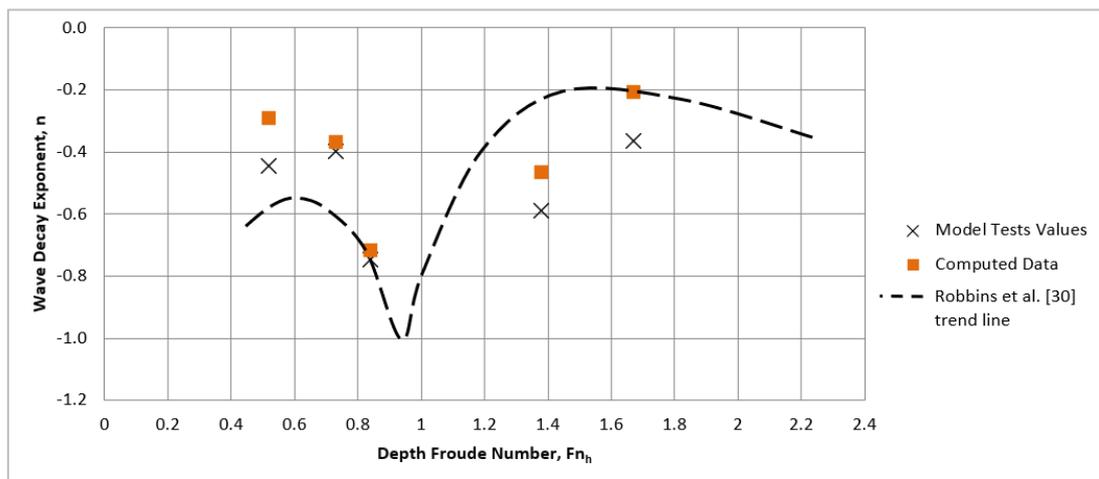
Fig. 25 Wave decay exponent trendline as a Function of Fn_h

Wake Wash of a Fast Small Boat in Restricted Waters: Ismail, M.A., Shaharuddin, N.M.R., Yaakob, O. B.,
Model Tests and Full-Scale Measurements   Jamal, M.H., Adnan, F.A., Rashidi, A.H.M., Azhary, W.A.H.W.M.,
Samion, M.K.H., Bachok, A., Ahmad, B., Ahmad, N.S.

Table 3 Wave Height Constant (γ) and wave Decay Exponential (n) at various Fn_h

	Fn_h	Wave Height Constant (γ)	Adjusted $(\pm1.35\%)$ (γ)	Computed (γ)	Exp (n)	Adjusted $(\pm2.89\%)$ Exp (n)	Computed Exp (n)
Sub-Critical	0.55	0.0275	0.0270	0.0259	-0.463	-0.446	-0.290
Trans-Critical	0.77	0.0441	0.0432	0.0430	-0.413	-0.398	-0.367
	0.88	0.0376	0.0368	0.0373	-0.774	-0.746	-0.717
Super-Critical	1.45	0.0299	0.0293	0.0260	-0.611	-0.589	-0.466
	1.75	0.0321	0.0315	0.0358	-0.377	-0.363	-0.206

Table 4 Comparison of Wave Decay Exponential (n) with Previous Studies at Various Fn_h

Exponent (n)	Current Computed Data (n)	Gadd [31]; Cox [32]; Macfarlane [21]	Kofoed-Hansen and Kirkegaard [33] Kofoed-Hansen [34]	Thomas et al. [29]	Doctors [35]	Doyle [36]
Sub-Critical	-0.290	-0.2 to -0.45		-0.2		-0.2
Trans-Critical	-0.367			↓	-0.7 to	↓
	-0.717					
Critical				-1.0	-1.06	-1.0
Super-Critical	-0.466		~-0.4	-0.2 to	-0.33 to	-0.2 to
	-0.206			-1.0	-0.5	-0.9

The wave exponent, n was compared with previous studies as summarized in Table 4 to show good agreement for this study's research values with differences of 6.25% to 20%. The obtained values can thus be used to predict the height of boat generated waves at desired lateral distances from the sailing line. This is beneficial to determining the wave wakes potential impact, energy transfer, and travel to the shoreline for criterion development in future.

3.2.2   Wave Decay at Finite Depth Linear Prediction

Waves behave differently during the shoaling process. Wave attenuation in finite depths is different from deep water conditions. In general, a wave envelope is a smooth curve that has its extremes outlined by an oscillating signal, which in this case study was boat wave wake. The purpose wave envelope analysis is to determine wave heights at locations where wave probes were not present, particularly the locations of the tide gauges used to acquire field measurements. During field work in Kilim River, tide gauges were placed 3 meters from the riverbank as in Figure 6, equivalent to 0.4m in the 1/7th scale model. Due to the nature (tripod stand) of the wave probes, wave probes could not be located at an equivalent distance. Instead, they were located at a distance of 1.2m as in Figure 12 during the model tests. Thus, to obtain the wave heights produced by the boat model at 0.4m, wave decay envelope estimation was carried out.

Super-critical, trans-critical and sub-critical categorized based on Fn_h conditions are associated with different wave crest propagation angles. To extrapolate the results to actual tide gauge measurements, estimations were made according to the wave crest propagation angles shown in Figure 26. In this study wave propagation angles (β) for the sub-critical and trans-critical condition ranged from 33° to 37° and wave propagation angles (β) for super-critical conditions ranged from 45° to 60°.

Ismail, M.A., Shaharuddin, N.M.R., Yaakob, O. B.,
Jamal, M.H., Adnan, F.A., Rashidi, A.H.M., Azhary, W.A.H.W.M.,
Samion, M.K.H., Bachok, A., Ahmad, B., Ahmad, N.S.

Wake Wash of a Fast Small Boat in Restricted Waters:
Model Tests and Full-Scale Measurements
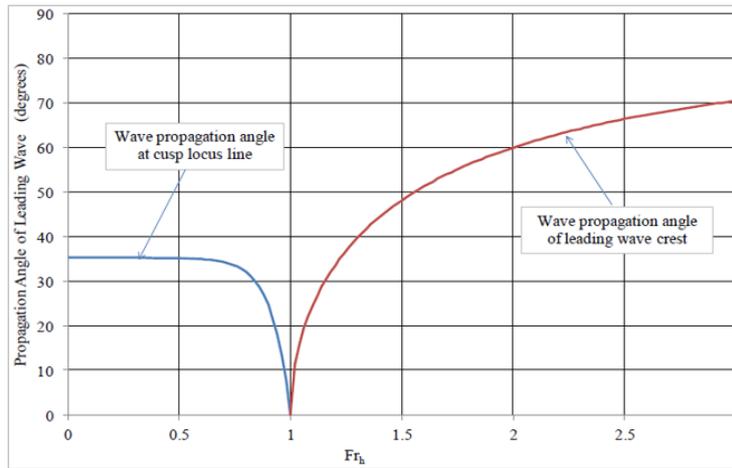
Fig. 26 Wave propagation angle β as a function of Fn_h [12]

Figure 27 shows the method used to determine the exact distance and the time taken for waves to reach the scaled down tide gauge distance from the shore of 0.4m. The prediction model of the wave decay envelope was simplified through the use of a linear decay line based on the finite depth wave decay study done by Sorenson [37], who found that wave amplitudes decay linearly with decreases in water depth as vessel waves travel farther from the sailing line. Wave decay rate was estimated using the wave height measured at wave Probe 6, which decayed linearly compared to either wave Probe 4 or Probe 5 located at the same distance and were parallel to the shore as shown in Figure 5. In Figure 26, the supercritical condition is illustrated using a blue line while the subcritical condition is shown using a red line. The trans-critical condition was similar to the sub-critical condition in that it interpolated data from wave Probe 4 to Probe 6. Boat routes or paths for both conditions were the same, but are shown slightly shifted to better differentiate between them.
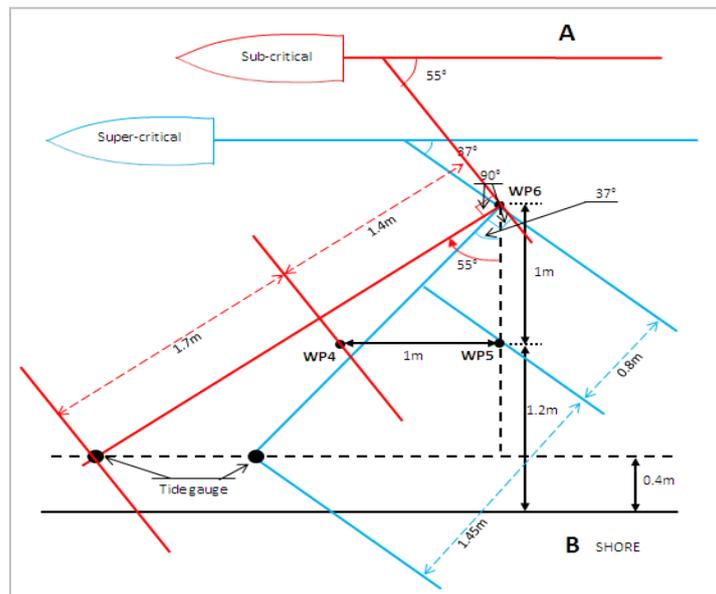
Fig. 27 Tide gauge location and wave angle at two conditions of sub-critical and super-critical

Wave Probe 2 and Probe 5 mirrored each other at different water depths. The wave heights obtained from Probe 5 showed a higher wave height than wave Probe 2 due to the shoaling effect. As the generated wave travelled from Probe 6 to Probe 4 or Probe 5 wave height decreased due to wave dispersion, as the wave was assumed to linearly decay. Using data from wave Probe 4, Probe 5, and Probe 6, wave heights at the location of the tide gauges used during

112

field-measurement were obtained through interpolation. Using the angle obtained from Figure 23, wave parameter travel under super-critical or sub-critical conditions was examined. Thus, distance and wave travel time were calculated. Figure 28 shows the wave decay envelope at a speed of 9.84knots. By using the time taken from the interpolation step shown in Figure 27, the required wave heights were obtained as shown in Table 5. The acquired wave data was based on a linear slope.
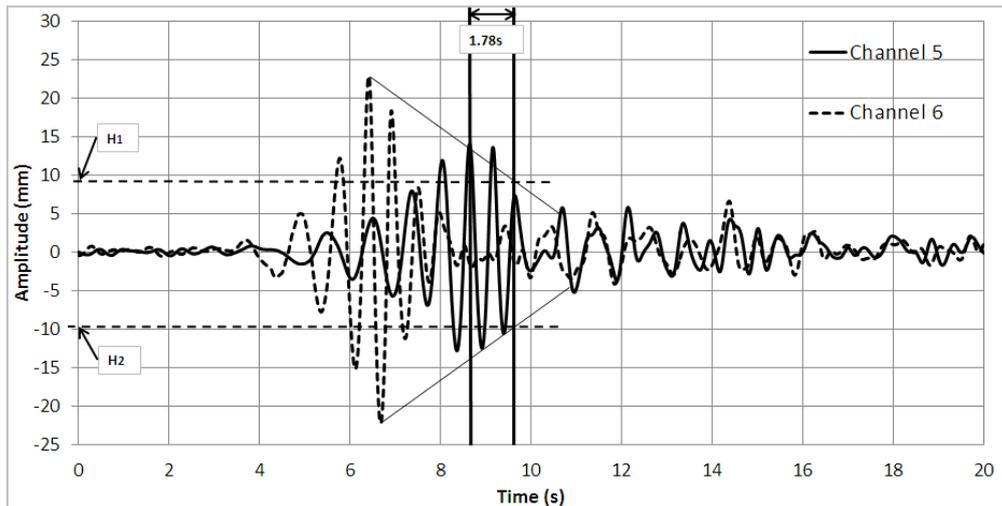
Fig. 28 Wave height and wave decay envelope analysis for a speed of 9.84knots

Table 5 Wave Height Results from the model tests (Wave Decay Envelope Method)

	Model Speed (knots)	Peak to Peak for Acquired Distance Time (s)	Tide Gauge for Acquired Distance Time (s)	H_1	H_2	Model Scale Wave Height (mm)	Full Scale Wave Height (m)
Sub Critical	2.59	2.54	2.03	8.5	6.0	14.5	0.102
Trans-Critical	3.63	1.58	1.28	12.0	11.5	23.5	0.165
	4.14	2.14	1.74	13.5	12.5	26.0	0.182
Super-Critical	6.84	2.22	1.78	10.0	6.5	16.5	0.116
	8.13	2.22	1.78	9.0	8.0	17.0	0.119
	8.26	2.24	1.79	7.0	6.0	13.0	0.091
	8.26	2.26	1.81	7.7	6.5	14.2	0.099
	9.82	2.28	1.82	8.0	7.0	15.0	0.105
	9.84	2.22	1.78	8.0	7.0	15.0	0.105

3.2.3   Wave Envelope Raw Data Visual (time domain) Comparison

A comparison of boat generated wave envelope patterns is shown in Figure 29, with model tests (top) and field measurements (bottom) indicating that the boat model produced wave wake patterns similar to actual boats in Kilim River, Langkawi. This suggests that the model results reflected the actual full-scale results.

Ismail, M.A., Shaharuddin, N.M.R., Yaakob, O. B.,
Jamal, M.H., Adnan, F.A., Rashidi, A.H.M., Azhary, W.A.H.W.M.,
Samion, M.K.H., Bachok, A., Ahmad, B., Ahmad, N.S.

Wake Wash of a Fast Small Boat in Restricted Waters:
Model Tests and Full-Scale Measurements
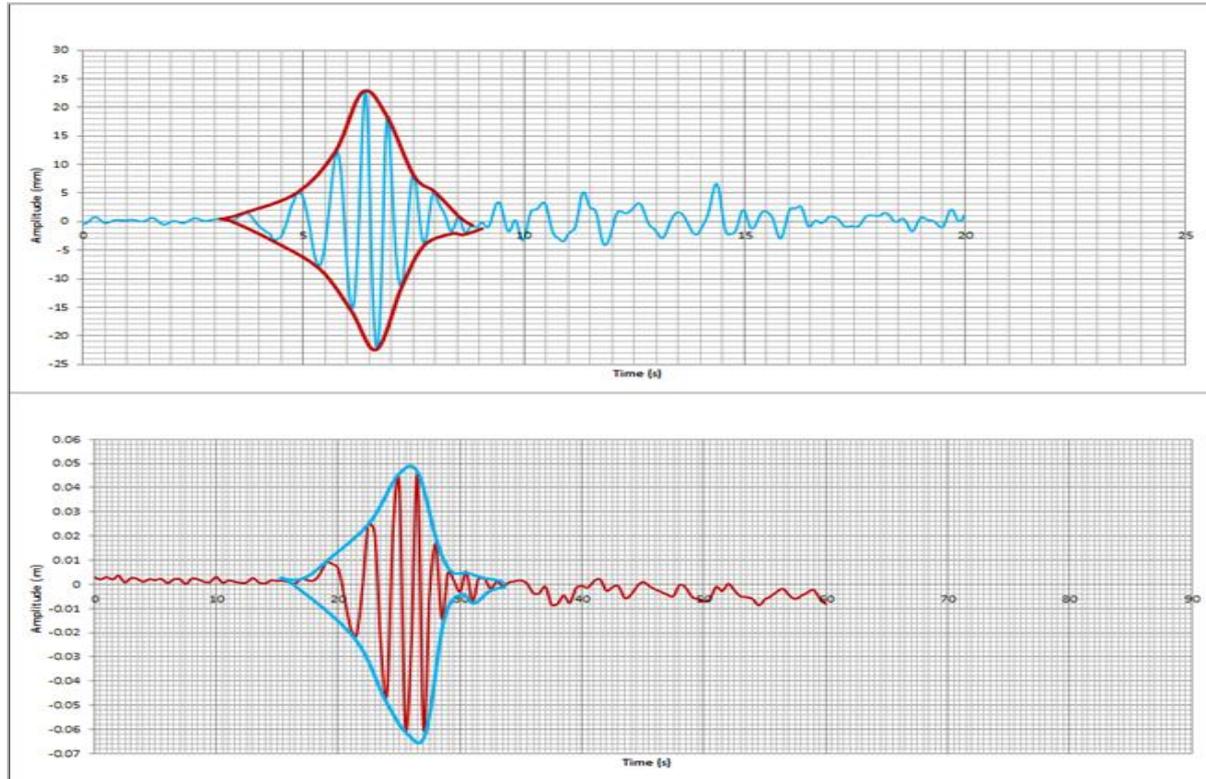
Fig. 29 Wave envelope for model tests and field measurements

3.3 International (Australia's Gordon River and Noosa River) Criterion Comparison

3.3.1 Maximum Allowable Wave Height Criterion

A comparison was made between measured data (model tests and field measurements) with the permissible 0.075m wave height criteria [38] used at Gordon River, Australia as a reference. To be able to compared with the criteria, normalized wave height data for the same sailing line distance were estimated by using Stumbo et al. [39] decay rate prediction formula at various Fn_h (as in Figure 30). 23m sailing line distance was used to compared the value between this model and full-scale experiment since the same sailing line distance were also used in the next section to determine the energy produced. Note that in this study, the model boats had full capacity of 11 people (equivalent to 715kg) onboard as explained in Section 2.3.

Figure 30 illustrates the boat generated wave in accordance to its depth Froude number (Fn_h) for sub, trans, and super-critical conditions. The Fn_h divisions were separated by blue dotted line. As mention in section 3.3, sub-critical, trans-critical and super-critical is associated to the displacement, semi-planing and planning mode respectively. Previously, sub-critical value is less than 0.75, trans-critical in the range between 0.75 to 1.00 while super-critical is larger than 1.0 by referring to Macfarlane research work [8]. However, for current study after normalizing the sailing line distance with the additional wave decay prediction for finite depth, the new sub-critical Fn_h value was found less than 0.65, the trans-critical range was from 0.65 to 0.95 and the super-critical Fn_h value was greater than 0.95. This change should be expected where the Froude number range shifted a bit occurred may be due to the variation of the high-speed craft hull form constructed as well as the wave formed from the amount immersed under water during the operating modes. The data obtained shows that at sailing line distance of 23m for model test and field measurement data, the boat produced wave heights smaller than 0.075m at Fn_h less than 0.5 under sub-critical condition. However, several points in both model testing and field measurement data indicates that the wave height were larger than 75mm from 0.5 to

0.65 Fn_h. This may be because of the transition from sub-critical into trans-critical mode, where the wake starts to increase in wave height as well as its energy.
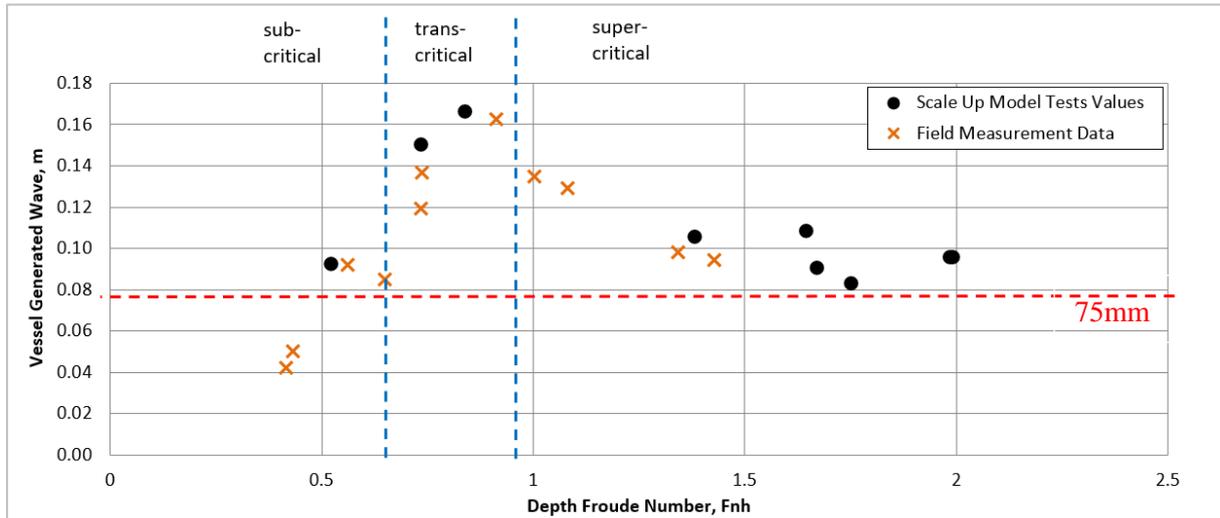
Fig. 30 27 feet boat wave wake height for boat with 11 people onboard at various Fn_h normalized at 23m sailing line distance

During the critical conditions, the Fn_h is 1. However, for this particular boat wave wake, the critical Fn_h occurred at 0.91 for the field measurements and 0.84 for model tests because the wave height already decreased when Fn_h became equal to 1. In super-critical conditions, the wave wake decreased as boat speed increased. At speeds of 15-20 knots (equivalent to 1.2 to 1.6 Fn_h), wave heights were reduced with 27.7% difference between the model test and field measurement data. The uncertainty in the model test data is not satisfactory due to the inability of the model boat to traverse a straight sailing line especially at super-critical condition. This is one of the limiting factors for model scale at this size during high-speed handling. As seen in Figure 30, wave wake heights measured during the trans-critical and super-critical region exceeded the allowable 75mm wave height (denoted by the red line) including some Fn_h of larger than 0.5. Only Fn_h below 0.5 complied with the wave wake criterion. In summary, the generated wave height for a boat with 11 people onboard exceeded the threshold criteria at speeds above 6knots equivalent to Fn_h of 0.5. In the next section, wave energy estimations further defined whether a certain boat wave height was considered safe or otherwise.

3.3.2   Maximum Allowable Wave Energy Criterion

By referring to one of the studies done by Macfarlane and Cox [6] in Noosa River that shows some similarity with Kilim River (in term of its vegetation, tidal current range, and steepness); for initial assessment the energy criterion should be less than 60 Joules/m for the riverbank to be safe from the erosion initiation. Wave wake energy estimation provides a comprehensive amount of the energy transferred against the riverbank. To assess the wave energy produced by the touring boat, wave energy consisting of kinetic and potential energy was summed according to the Airy theory; Potential and kinetic energy components are equal if the potential energy is calculated relative to the still water level (SWL) and all waves propagate in the same direction, thus the total wave energy in one wavelength per unit crest width is given by $E = \frac{\rho g H^2 L}{8}$. Since the wave measured under deep water condition, the wave length, L became $\frac{gT^2}{2\pi}$. Thus the transmitted wave energy, E for each wavelength (per unit width of wave crest) was estimated using Equation 3 [8]:

$$E = \frac{\rho g^2 H^2 T^2}{16\pi} \tag{3}$$

Where:

E = Wave energy (Joules/m)

ρ = Water density (kg/m^3)

H = Maximum Wave height (m)

T = Wave period (s) of the corresponding maximum wave height

Figure 31 shows the wave energy produced by the wake wave of the Kilim River 8.23m touring boat at full carrying capacity of 10 passenger plus one boat operator onboard at several tested speed or Fn$_h$ conditions.

The wave energy is calculated based on both full measurement and model test data. It can be noted from the calculated energy as in Figure 31, almost all energy exceeds the allowable energy of 60 Joules/m except at the Fn$_h$ of less than 0.45 and a few at Fn$_h$ larger than 1.65. It can be seen that for the Fn$_h$ of less than 0.45, the wave wake is considered safe as both the wave height and wave energy criterion as shown in Figures 30 and 31 show that under this sub-critical condition or displacement operating mode, the wave height produced will considered having no harm to the riverbank. The quantity of energy calculated for a higher speed at Fn$_h$ greater than1.34 was found to be near to the permissible limit of 60Joules/m. The difference is calculated to be between 1% and 30% lower or higher. Although some of the wave energy was found to be safe at some points during this super-critical or planing mode, the boat still required to enter trans-critical region of semi-planing mode, where the wave wake generated is the worst at this condition and did not meet any of the wave height or energy criterion, as shown in Figures 30 and 31.

Based on this finding, the current operation for full carrying capacity of the 8.23m boat does not meet the wave energy criterion for the Fn$_h$ range of 0.5 to 1.65. As the riverbank strength is started to weaken upon impact of these destructive waves. Furthermore, the waves parameter allowed should not be assessed only by the wave wake height it produced; instead, both wave height and its corresponding period it produced under several operating condition must be counted.
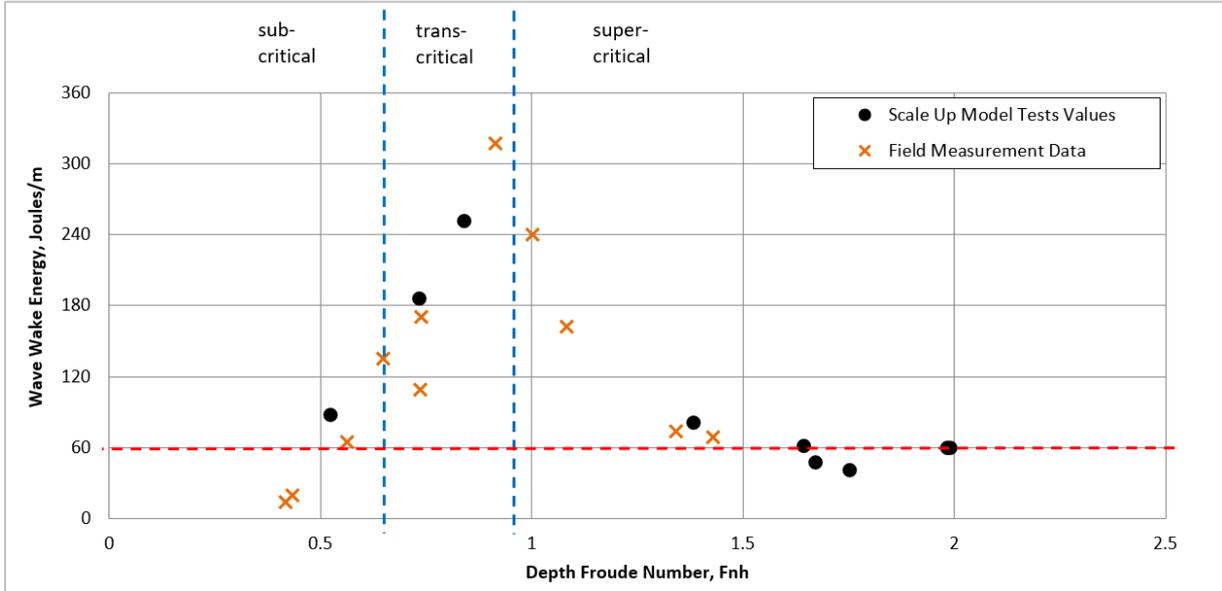
Fig. 31 Wave energy per maximum wave height for a boat with 11 people onboard

4. Conclusions

Assessments were carried out to determine the Kilim River most used touring boat wave wake characteristics through full scale measurement and model testing approach at NAHRIM facility. In general, there were many related parameters to characterized the wave wake produced. Priority given to the maximum wave height produced under certain speeds at deep water condition. The non-dimensional attenuation data produced from the value obtained under this deep-water condition is beneficial to full scale boat wake assessments and allows future investigations to be made for limited riverbank widths or for areas with limited field work accessibility. To recap, the exponential value, n of the 8.23m boat was predicted to be in the range of -0.36 to -0.75 under various operating mode. On top of that the water depth effect to the wave height produced were studied via the prediction of the wave attenuation; valid for extrapolating wave data linearly at finite water depths over simplified bank slope.

Under a permissible wave height criterion of 75mm in reference to Gordon River showed that Kilim River touring boat wave wakes were safer only during sub-critical conditions. Wave magnitude was shown highest during trans-critical approaching critical conditions. For a boat with 11 people onboard, it is suggested that boat speed should be below 5.4knots to avoid harming the riverbanks. Energy on the other hand, was quantified using the energy per maximum wave height approach. Nearly all measured results as in Figure 31 showed that boat generated wave energy exceed the threshold of 60Joules/m except the speed of less than 5.4knots that equivalent to 0.43 Fn_h similar to the wave height allowable approach. Based on the data shown in Figure 31, the wave wake energy should be maintained below 0.40 Fn_h or 5knots to be safe. Both wave height and energy criterion approach results in that touring boat should be operated under displacement mode on the critical boat route that still suffered from a severe riverbank erosion.

The wave energy data might not include all the operating mode values variation. However, based on the presented data, it intended to benefit the related bodies in reducing the adverse effect of the touring boat wave wake to the riverbank. It can be implemented by enforcing a much lower cruising speed for the touring boat movement at the critical location. This wave wake energy assessment was based on energy criterion used at the Noosa River, which had an environment and vegetation similar to the current research area conditions. These rivers of Noosa River and Kilim River are also similar in their compact shorelines and sheer soil banks, which were used as benchmark on the allowable maximum wave wake height and energy. However, there may be some dissimilarity in their actual results. Therefore, extensive studies should be conducted in the future to find the applicable wave wake criteria for Kilim River, Langkawi.

ACKNOWLEDGEMENTS

REFERENCES

[1]   Blount, D. L., 1993. Reflections on planing hull technology. *Centennial*, 1893-1993.

[2]   Radojčić, D., Kalajdžić, M., Simić, A., 2019. Power Prediction Modeling of Conventional High-Speed Craft. *Springer International Publishing*. https://doi.org/10.1007/978-3-030-30607-6

[3]   Johnson, S., 1994. Recreational Boating Impact Investigations Upper Mississippi River System, *Pool 4 Red Wing*, Minnesota, USA.

[4]   Kirkegaard, J., Kofoed-Hansen, H., Elfrink, B., 1999. Wake wash of high-speed craft in coastal areas. *Coastal Engineering*, 1998. 325-337. https://doi.org/10.1061/9780784404119.023

Ismail, M.A., Shaharuddin, N.M.R., Yaakob, O. B.,   Wake Wash of a Fast Small Boat in Restricted Waters:
Jamal, M.H., Adnan, F.A., Rashidi, A.H.M., Azhary, W.A.H.W.M.,   Model Tests and Full-Scale Measurements
Samion, M.K.H., Bachok, A., Ahmad, B., Ahmad, N.S.

[5]   Nanson, G. C., Von Krusenstierna, A., Bryant, E. A., Renilson, M. R., 1994. Experimental measurements of river-bank erosion caused by boat-generated waves on the gordon river, Tasmania. *Regulated Rivers: Research & Management*, 9.1, 1-14. https://doi.org/10.1002/rrr.3450090102

[6]   MacFarlane, G. J., Cox, G. "The development of wave wake criteria for the Noosa and Brisbane Rivers in South East Queensland." In Fith International Conference on Coastal Environment 2004, vol. 10, pp. 55-72. (2004).

[7]   Ahmad, M. F., Yusoff, M. M., Husain, M. L., Nik, W. W., 2011. An investigation of boat wakes wave energy: a case study of Kemaman river estuary. In *Universiti Malaysia Terengganu International Annual Symposium*. UMTAS, Kuala Terengganu, 907-913.

[8]   Macfarlane, G. J., 2012. Marine vessel wave wake: focus on vessel operations within sheltered waterways. PhD thesis, University of Tasmania, Austalia. https://doi.org/10.5957/SMC-2012-A06

[9]   La, T.V., Yagisawa, J., Tanaka, N., 2014. Reinforcing Riverbank Stability by Vegetation Under Boat-Generated Wave Attacks. Proceedings of the 19th IAHR-APD Congress 2014, Hanoi, Vietnam. 1-8.

[10]   Cox, G., Macfarlane, G., 2019. The effects of boat waves on sheltered waterways-thirty years of continuous study. Australasian Coasts and Ports 2019 Conference: Future directions from 40 [degrees] S and beyond, Hobart, Engineers Australia.

[11]   Bilkovic, D. M., Mitchell, M. M., Davis, J., Herman, J., Andrews, E., King, A., Mason, P., Tahvildari, N., Davis, J., Dixon, R. L., 2019. Defining boat wake impacts on shoreline stability toward management and policy solutions. *Ocean & Coastal Management*, 182, 104945. https://doi.org/10.1016/j.ocecoaman.2019.104945

[12]   Novak, P. A., Fairfield, C. A., Miloshis, M., Knight, Z. C., Lindsay, R., King, A. J. 2020. Bank erosion in a macrotidal tropical river: Exploring the relative impact of boat wash on riverbank erosion. *River Research and Applications*, 37(1), 3-16. https://doi.org/10.1002/rra.3736

[13]   Kurata, K., Oda, K., 1985. Ship waves in shallow water and their effects on moored small vessel. *Coastal Engineering*, 1984, 3258-3273. https://doi.org/10.1061/9780872624382.219

[14]   Ghani, M. P. A., Rahim, M. A. R. M. A., 2008. The prediction of wake wash in the towing tank. Jurnal Mekanikal 26(2).

[15]   Ozdemir, Y. H., Cosgun, T., Barlas, B., 2021. Wave Field Generated by Finite-Span Hydrofoils Operating beneath a Free Surface. *Brodogradnja: Teorija i praksa brodogradnje i pomorske tehnike*, 72(1), 145-167. https://doi.org/10.21278/brod72108

[16]   Benassai, G., Piscopo, V., Scamardella, A., 2013. Field study on waves produced by HSC for coastal management. *Ocean & coastal management*, 82, 138-145. https://doi.org/10.1016/j.ocecoaman.2013.06.003

[17]   Maynord, S. T., 2005. Wave height from planing and semi-planing small boats. *River Research and Applications*, 21(1), 1-17. https://doi.org/10.1002/rra.803

[18]   Robbins, A. W., 2013. Shallow water catamaran wash: simple characterisations for a complex phenomenon. PhD thesis. University of Tasmania, Australia.

[19]   Ahmed, T. M., Elaghbash, A. O., Banawan, A. A., Ahmed, Y. M., Hassan, A. M., 2020. Numerical Prediction of Solitary Wave Formation of a Planing Hull in Shallow Water Channels. *Brodogradnja: Teorija i praksa brodogradnje i pomorske tehnike*, 71(3), 135-148. https://doi.org/10.21278/brod71308

[20]   Havelock, T. H., 1908. The propagation of groups of waves in dispersive media, with application to waves on water produced by a travelling disturbance. Proceedings of the Royal Society of London. Series A, Containing Papers of a Mathematical and Physical Character 81(549), 398-430. https://doi.org/10.1098/rspa.1908.0097

[21]   Macfarlane, G. J., 2002. The measurement and assessment of sub-critical vessel generated waves.

[22]   Renilson, M. R., Lenz, S. 1988. An Investigation into the Effect of Hull Form on the Wake Wave Generated by Low Speed Vessel's. Ship Hydrodynamics Centre Report, Australian Maritime College, Tasmania.

[23]   Cox, G. L., Gregor Macfarlane. 2019. The effects of boat waves on sheltered waterways–thirty years of continuous study. Proceedings of Australasian Coasts & Ports Conference 2019. Engineers Australia.

[24]   Ziylan, K, Nas. S., 2016. A Study On The Effects Of Trim Optimisation On Ship Resistance Of A Sub-Panamax Type Container Vessel. Proceedings Book, 24.

[25]   MAXSURF Resistance Wake and Power Prediction, 2016. MAXSURF Integrated Naval Architecture Software for all Types of Vessels. https://www.maxsurf.net/resistance.html accessed 6th February 2016.

Wake Wash of a Fast Small Boat in Restricted Waters: Ismail, M.A., Shaharuddin, N.M.R., Yaakob, O. B.,
Model Tests and Full-Scale Measurements Jamal, M.H., Adnan, F.A., Rashidi, A.H.M., Azhary, W.A.H.W.M.,
Samion, M.K.H., Bachok, A., Ahmad, B., Ahmad, N.S.

[26] Elhadad, A., Duan, W. Y., Deng, R., Elhanfey, H., 2014. Numerical Analysis for Resistance Calculations of NPL as a Floating Hull for Wave Glider. *Applied Mechanics and Materials*. 619. Trans Tech Publications Ltd. https://doi.org/10.4028/www.scientific.net/AMM.619.38

[27] Macfarlane, G. J., Bose, N., Duffy, J. T., 2014. Wave wake: focus on vessel operations within sheltered waterways. *Journal of Ship Production and Design*, 30(3), 109-125. https://doi.org/10.5957/JSPD.30.3.130055

[28] Wang, P., 2016. Material Dispersion by Ocean Eddies and Waves. PhD thesis, University of Miami, USA.

[29] Thomas, G.A., MacFarlane, G.J., Dand, I., Robbins, A., Renilson, M.R., 2007. The decay of catamaran wave wake in shallow water. In FAST: International Conference on Fast Sea Transportation, 1, 184-192.

[30] Robbins, A., Thomas, G., Macfarlane, G. J., Renilson, M. R., Dand, I., 2007. The decay of catamaran wave wake in shallow water. In 9th International Conference on Fast Sea Transportation, Shanghai, China.

[31] Gadd, G. E., 1994. The wash of boats on recreational waterways.

[32] Cox, G., 2000. Sex, lies and wave wake. In The Royal Institution of Naval Architects, RINA, Proceedings of the International Conference Hydrodynamics of High Speed Craft Wake Wash & motions Control, London, UK, ISBN: 0 903055 62 7. Paper: P2000-4 Proceedings.

[33] Kofoed-Hansen, H., Kirkegaard, J., 1996. Technical investigation of wake wash from fast ferries. Danish Hydraulic Institute, Hørsholm, Denmark 41.

[34] Kofoed-Hansen, H., 1997. Wake wash from fast ferries in Denmark. In FAST'97 Conference Papers, Sydney, Australia, 471-478.

[35] Doctors, L. J., 2001. The generation and decay of waves behind high-speed vessels. In Proceedings of sixteenth international workshop on water waves and floating bodies (16 IWWWFB), Hiroshima, Japan, 33-36.

[36] Doyle, R., 2001. An investigation into the wake wash of high-speed ferries in shallow water. PhD thesis, Queen's University of Belfast, Ireland.

[37] Sorensen, R. M., 1973. Water waves produced by ships. 9754. https://doi.org/10.1061/AWHCAR.0000187

[38] Bradbury, J., 2005. Revised wave wake criteria for vessel operation on the lower Gordon River. Unpublished Nature Conservation Branch Report, Tasmania Department of Primary Industry, *Water & Environment*. Retrieved from http://tas. gov. au

[39] Stumbo, S., Fox, K., Dvorak, F., Elliot, L., 1999. The prediction, measurement, and analysis of wake wash from marine vessels. *Marine Technology and SNAME News*, 36(4), 248-260. https://doi.org/10.5957/mt1.1999.36.4.248

Submitted: 14.11.2021. Mohd Arif Ismail[a]
Nik Mohd Ridzuan Shaharuddin[a,b] ; ridzuan@mail.fkm.utm.my
(corresponding)
Omar Yaakob[b]
Mohamad Hidayat Jamal[c]
Faizul Amri Adnan,[b]
Ahmad Hadi Mohamed Rashidi[d]
Wan Ahmad Hafiz Wan Mohd Azhary[d]
Mohd Kamarul Huda Samion[e]
Andiknurdiyana Bachok[a]
Badruzzaman Ahmad[a]
Nur Shafira Ahmad[a]

a. School of Mechanical Engineering, Faculty of Engineering, Universiti Teknologi Malaysia, 81310 UTM Skudai, Johor Malaysia
b. Marine Technology Center (MTC), Universiti Teknologi Malaysia, 81310 UTM Skudai, Johor Malaysia
c. School of Civil Engineering, Faculty of Engineering, Universiti Teknologi Malaysia, 81310 UTM Skudai, Johor Malaysia
d. Centre for Coastal and Oceanography Studies, National Hydraulic Research Institute of Malaysia
e. Hydraulic & Instrumentation Laboratory, National Hydraulic Research Institute of Malaysia

Accepted: 28.04.2022.